Title

From nanoscale interface characterization to sustainable energy storage using all-solid-state batteries.

Journal

Nature nanotechnology, 15(3)

ISSN

1748-3387

Authors

Tan, Darren HS
Banerjee, Abhik
Chen, Zheng
et al.

Publication Date

2020-03-01

DOI

10.1038/s41565-020-0657-x

Peer reviewed

REVIEW ARTICLE
https://doi.org/10.1038/s41565-020-0657-x

nature nanotechnology

From nanoscale interface characterization to sustainable energy storage using all-solid-state batteries

Darren H. S. Tan[1], Abhik Banerjee[1], Zheng Chen[1,2,3] ✉ and Ying Shirley Meng[1,3] ✉

The recent discovery of highly conductive solid-state electrolytes (SSEs) has led to tremendous progress in the development of all-solid-state batteries (ASSBs). Though promising, they still face barriers that limit their practical application, such as poor interfacial stability, scalability challenges and production safety. Additionally, efforts to develop sustainable manufacturing of lithium ion batteries are still lacking, with no prevailing strategy developed yet to handle recyclability of ASSBs. To date, most SSE research has been largely focused on the discovery of novel electrolytes. Recent review articles have extensively examined a broad spectrum of these SSEs using evaluation factors such as conductivity and chemical stability. Recognizing this, in this Review we seek to evaluate SSEs beyond conventional factors and offer a perspective on various bulk, interface and nanoscale phenomena that require urgent attention within the scientific community. We provide a realistic assessment of the current state-of-the-art characterization techniques and evaluate future full cell ASSB prototyping strategies. We hope to offer rational solutions to overcome some major fundamental obstacles faced by the ASSB community, as well as potential strategies toward a sustainable ASSB recycling model.

The past several decades have seen conventional lithium ion batteries (LIBs) dominate the portable devices and consumer electronics market. Today, LIBs are gradually penetrating other technologies including electric vehicles and grid storage. The success of LIBs stems from the rapidly growing efforts in battery research and development, leading to vast improvements in materials performance and decrease in production costs. However, the justification for a more widespread adoption of LIBs entails overcoming fundamental obstacles such as safety hazards from battery fires and explosions, meeting the demand for higher energy density and achieving satisfactory performance in a wider temperature range for application in various climate conditions. In view of these concerns, all-solid-state batteries (ASSBs) are regarded as one of the future energy storage technologies that can compete with the state-of-the-art LIBs. Owing to the use of non-flammable solid-state electrolytes, ASSBs are well-placed to effectively eliminate battery safety concerns in electric vehicles, airline industry and grid storage applications in urban environments. Their wide operating temperature range also drastically reduces cooling power requirements with immediate benefits on costs and energy efficiency. While energy densities of ASSBs are virtually identical to those of LIBs at the materials level, they can be potentially increased by 50% or greater at the pack and system level from utilizing stackable formats without the need for individual cell packaging, reinforced metallic casings, or allocated space for coolants.

Despite their many promising benefits, ASSBs still face a multitude of barriers before they can be transferred from the laboratory to commercial manufacturing lines (Fig. 1). In our view, the most pressing challenges are: (1) solid-state-electrolyte (SSE) chemistry: to date, no single SSE can meet the combination of properties necessary for commercialization, that is high ionic conductivity, ease of processability and wide electrochemical stability among others; (2) characterization challenges: ASSBs are inherently difficult to characterize given the buried and heterogenous nature of their interfaces, as well as their sensitivity toward electron beam damage; (3) scalable design: despite recent advances[1,2], air sensitivity and the poor mechanical properties of SSEs still pose challenges in implementing roll-to-roll processability for scalable ASSB fabrication; and (4) sustainability: no ASSB recycling models exist yet—any sustainable ASSB model would require cell level recycling strategies beyond electrodes recovery. In this Review, we will take a close look at each of these obstacles and offer our perspective on how to approach them.

Solid state electrolyte chemistry

Scientists have recently discovered a plethora of SSE materials with ionic conductivities greater than 10^{-2} S cm^{-1} at 25°C, comparable to that of liquid electrolytes[3]. However, high ionic conductivity alone is not sufficient to make cells practical. Recent reports on highly conductive oxide- or sulfide-based SSEs show that poor interfacial stability makes them impractical[3]. Such instability arises from two types of reactions: (1) interfacial reactions between the electrode and SSE, which occur spontaneously upon physical contact and (2) electrochemical decomposition of the SSE itself during cell cycling at high voltage. Although some oxide-based electrolytes such as those from the garnet and NASICON class can be stable over a wide range of voltages[4], this voltage window is still not satisfactory. Figure 2a illustrates the electrochemical stability windows of some SSEs compared to common electrode materials. Although polymer-composite-based SSEs represent an important class of materials for solid-state batteries, these materials have already been extensively covered in recent review articles[5–7]. Thus, we will focus on inorganic solid electrolytes, which are comparatively novel and not as well understood. In this section, we discuss the fundamentals

[1]Department of NanoEngineering, University of California San Diego, La Jolla, CA, USA. [2]Program of Chemical Engineering, University of California San Diego, La Jolla, CA, USA. [3]Sustainable Power & Energy Center (SPEC), University of California San Diego, La Jolla, CA, USA.
✉e-mail: zhengchen@eng.ucsd.edu; shmeng@ucsd.edu

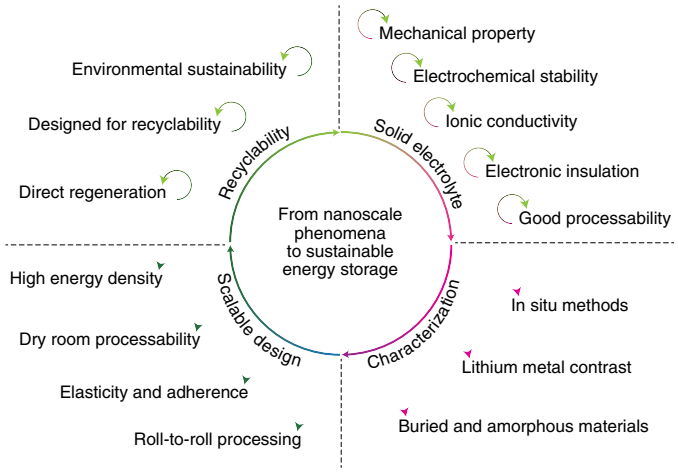

Fig. 1 | Solid-state batteries development. Summary of major scientific challenges.

of each type of interfacial reaction and evaluate the methods to prevent them.

Cathode interfacial reactions. The first type of interfacial chemical reaction stems from intrinsic chemical reactivity between the high-voltage cathodes and SSEs[8,9]. These spontaneous reactions result in the formation of transition metal oxides, sulfides, phosphates and other undesirable products on the cathode–SSE interface that increase cell polarization and limit rate capability. Oxide anions from the layered transition metal oxides form stronger electrostatic attractions with lithium ions than sulfide anions due to the hard–soft acid–base principle. Thus, transfer of Li^+ from sulfides to oxides occurs until equilibrium is reached, thickening the resistive layer and suppressing any ionic conduction across the interface. As the transfer of Li^+ from sulfide to oxide anions is charge balanced by the electronic conductive network of the cathode material, the most natural approach to prevent this effect is to adopt an electronically insulating but ionically conductive coating layer at the SSE–cathode interface. Protective coating materials such as Li_2SiO_3, $Li_4Ti_5O_{12}$ (LTO), $LiTaO_3$, $LiAlO_2$, Li_2O-ZrO_2, and $LiNbO_3$ (LNO) have been proposed[10]. For example, a 20-nm-thick LTO coating on $LiCoO_2$ (LCO) could reduce cathode interfacial resistance by an order of magnitude compared to the uncoated cathode[11]. In another example, an LNO coating of thickness as low as 5 nm was adequate to prevent interfacial reactions[12].

Protective coatings on the cathode can also alleviate cation interdiffusion problems along the SSE–cathode interface. Cation interdiffusion occurs from exchange between the transition metal ions and SSE cations. Interdiffusion can occur over spatial scales of up to 100 nm, forming a highly resistive layer that blocks Li^+ from crossing the interface. Interdiffusion energies at the LCO (110) and β-Li_3PS_4 (010) interface have been calculated and it has been found that Co and P ion diffusion exchange is highly thermodynamically favourable[13]. Adopting a protective layer such as LNO can prevent the Co and P interdiffusion, as Nb and P interdiffusion are slow due to the strong bonds between Nb and O anions. Such protective layers were later experimentally validated with transmission electron microscopy (TEM), where long range Co distribution was tracked at the interface protected by a Li_2SiO_3 coating[14].

Despite these results, there is still a lack of consensus on how to select protective coating materials. For example, incorporation of a charge carrier (such as in $LiAlO_2$) in Al_2O_3 improves cell efficiency,[15,16] most likely because of the energetically favourable activation of Al_2O_3 with Li^+ from the cathode during cell cycling. This was experimentally supported by the effectiveness of an Li_2SiO_3 coating on LCO in improving the cell rate performance compared to SiO_2[14]. Regardless of the material, any coating must be sufficiently thin to avoid negative impacts on cell impedance, as oxides often exhibit low ionic conductivities (for example, 10^{-8} S cm^{-1} for LTO). Therefore, more conductive (~10^{-6} S cm^{-1}) phosphate-based coating materials, such as lithium thiophosphate (LPS), have been proposed; these exhibit both high theoretical oxidative stability and low ion migration barriers[17]. As experimentally shown for the NCM811–LPS interface, oxide cathodes tend to react with PS_4^{3-} groups in sulfide-based SSEs due to the exchange of O and S atoms between the SSE and the cathode to form PO_4^{3-} units[18]. Because the bond dissociation energy of a P–O bond (597 kJ mol^{-1}) is larger than that of P–S bonds (346 kJ mol^{-1}), O–S exchange is highly favourable. Thus, the reactivity of phosphate-based coating materials in which P atoms are already bonded to O atoms is expected to be low.

Anode interfacial reactions. In general, there are two kinds of interfaces formed between SSEs and lithium metal: ionically conductive and mixed conductive ones. For example, $Li_{10}GeP_2S_{12}$ (LGPS) has an ionic conductivity greater than 10^{-2} S cm^{-1} and decomposes upon contact with lithium metal,[4] forming Li_2S (an insulator), Li_3P (an ionic conductor) and an Li–Ge alloy (an electronic conductor); collectively making the interface a mixed conductor[19]. Because of the presence of a conductive component, as the interface grows, the anode impedance increases until cell failure. The same principles apply for Si-, Sb-, Sn- and As-containing SSEs, as they also form electronically conductive alloys with lithium. As such, despite their high ionic conductivity, these electrolytes are not suitable for lithium metal ASSBs. On the other hand, LPS-based glasses or glass ceramics ($xLi_2S.yP_2S_5$), along with argyrodite-based SSEs (Li_6PS_5X; X = Cl, Br, I) are more stable. When these SSEs meet lithium metal, their decomposed products include Li_2S, Li_3P, and LiX (X = Cl; Br, I), which are all electronically insulating,[4] thus passivating the SSE interface.

Room temperature long cycle performance of lithium metal ASSBs still remains challenging. One reason is the difficulty of maintaining good wettability at the lithium–SSE interface during cell cycling in order to achieve homogenous and dense lithium plating. In an effort to overcome this problem, conformal alumina coating on lithium has been shown to reduce interfacial resistance by almost two orders of magnitude in oxide-based SSEs[20]. However, such treatments are only feasible with garnet and other oxide-based SSEs due to their better chemical stabilities against lithium. For sulfide-based SSEs, any high temperature treatment would promote unwanted reactions and form a thick solid electrolyte interface (SEI) that renders cells unusable. While some studies demonstrated good lithium–SSE contact by simple cold pressing[21,22], the effectiveness of this methodology in lowering interfacial resistance and allowing uniform lithium plating especially in long term cell cycling is still unclear. Another solution could be the use of a thin Li^+ conductive polymer layer between the lithium anode and the SSE. This strategy was previously shown to enable extended cell cycling in Li|polyethylene oxide (PEO)|$Li_7La_3Zr_2O_{12}$ (LLZO) and Li|PEO|β-LPS configurations[23,24]. However, using conductive polymers often requires cells to be cycled at elevated temperatures. The good cyclability of these cells is often attributed to PEO's ability to either protect lithium or achieve good wettability. Even though there have also been reports of bare Li|SSE cell configurations showing good cell cyclability at elevated temperatures[25,26], practical devices must be operated at room temperature. Prevailing theories suggest that lithium dendrites propagate as a result of deposition within pores near the lithium–SSE interface[27], with experimental reports observing lithium deposits originating from pores at the interface that propagate along grain boundaries due to inhomogeneous current distribution[28]. However, studies using grain-free single crystal

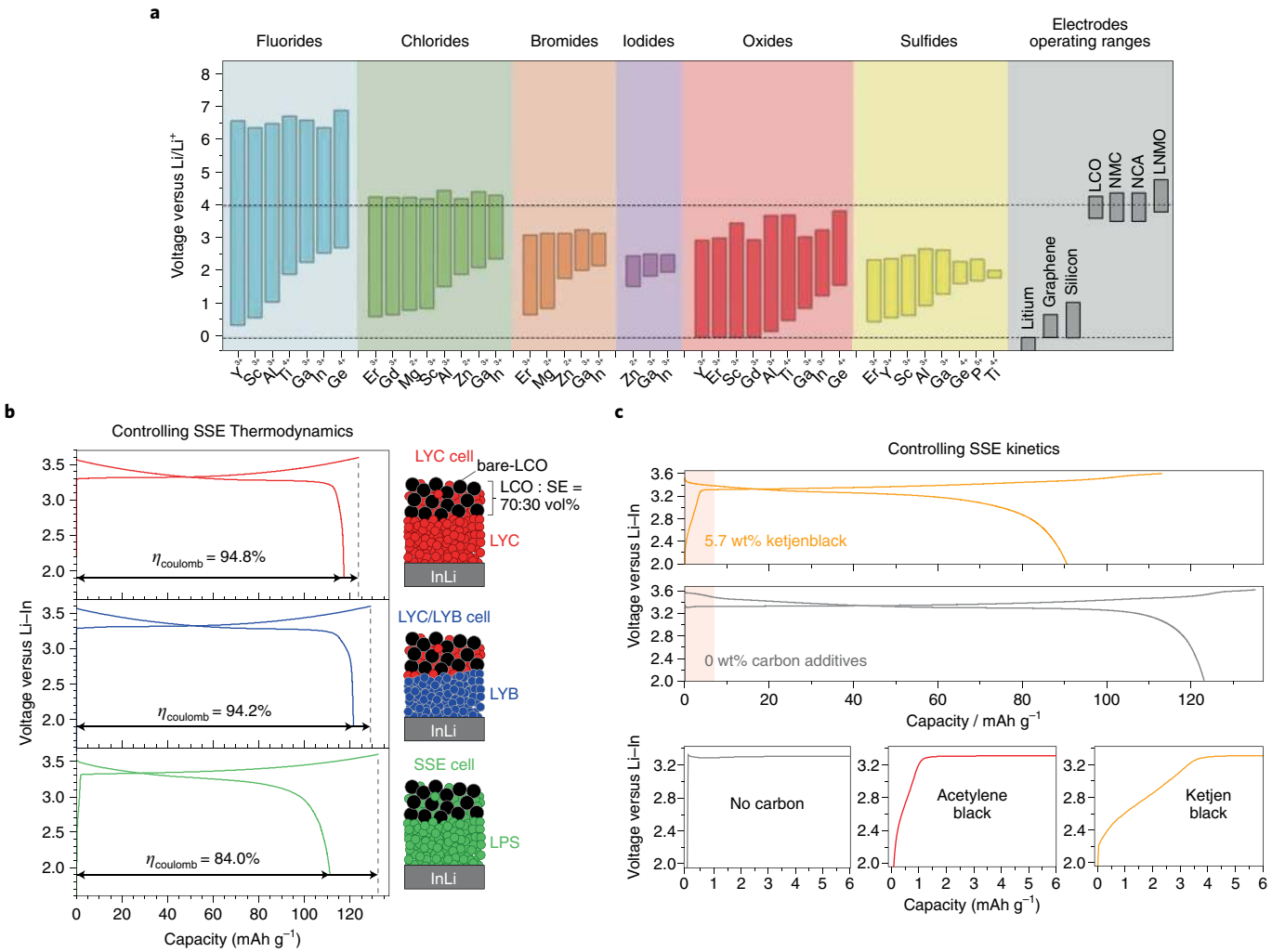

Fig. 2 | Electrochemical stability of various solid electrolytes and their effects on cell performance. a, Illustration of solid electrolytes stability windows versus common electrodes typical operating potential. LCO, lithium cobalt oxide; NMC, nickel manganese cobalt; NCA, nickel cobalt aluminium; LNMO, lithium nickel manganese oxide. **b**, Methods to improve thermodynamic stabilities of solid electrolytes, by using a solid electrolyte of higher oxidation stability. LYC, Li_3YCl_6 solid electrolye; LYB, Li_3YBr_6 solid electrolyte. **c**, Methods to control decomposition kinetics of solid electrolytes, by using carbon with lower specific area. Adapted with permission from refs. [36,85], Wiley-VCH Verlag GmbH & Co. KGaA (**a** and **b**, respectively); and ref. [42], American Chemical Society (**c**).

$Li_6La_3ZrTaO_{12}$ also reported lithium penetration through the SSE[29]. Interestingly, only lithium phosphorous oxynitride (LiPON) appear to be able to effectively prevent lithium dendrite formation and enable cell cyclability beyond 10,000 cycles[30,31]. It is probably the amorphous, conformal and virtually defect free nature of the material that is responsible for such performances.

In spite of the challenges faced at the anode interface, metallic lithium is still indispensable to increase energy densities of ASSBs. Moreover, lithium metal ASSBs can potentially be used in an anode-free configuration. Such ASSBs have been demonstrated in thin film formats nearly two decades ago in a LiPON|LCO battery[30]. Here, surface passivation in solid electrolytes prevents side reactions from continuously forming, allowing retention of the lithium reservoir within the cell after the first charge cycle. This situation differs fundamentally from that in liquid electrolytes where continuous formation of new SEI and dead lithium at each cycle requires sacrificial lithium replenishment[32]. Adoption of anode-free cell configurations would immensely simplify large scale ASSB processing and lower its cost, because it would eliminate sophisticated lithium metal lamination and interface treatment steps, especially when lithiophobic SSEs are used[33]. However, the same challenges encountered in other lithium metal ASSBs, such as dendritic cell shorting, also apply in anode-free cell configurations.

SSE electrochemical decomposition. Despite the fact that protective coating layers can effectively reduce interfacial reactions, they cannot prevent interfacial electrochemical decomposition. Electrochemical decomposition during cell charging is an unavoidable intrinsic thermodynamic phenomenon of the SSE. The SSE at each electrode experiences a strong oxidative or reductive environment that leads to the formation of unwanted interfacial products, resulting in poor first cycle Coulombic efficiencies and high impedance growth. To reduce the effects of electrochemical decomposition, SSE thermodynamics can be altered through compositional changes. For instance, introducing oxygen dopants stabilizes the electrolyte, because oxides are more thermodynamically stable than sulfides due to their lower anion polarization. In one study, P_2O_5 was introduced in place of P_2S_5 during SSE synthesis, forming oxygenated units within the bulk Li_3PS_4 glass ceramic oxysulfide system[34]. The electrochemical stability window of oxysulfides with the

composition $Li_{10}GeP_2S_{12-x}O_x$ (LGPS) is wider than that of the oxygen-free counterpart, with only a small trade-off in bulk ionic conductivity[35]. Alternatively, SSE thermodynamics can be controlled by using different SSEs with suitable redox stability at each electrode. Figure 2b compares the improvements in first cycle Coulombic efficiency by using SSEs with higher oxidative stability. For example, halide-based Li_3YCl_6 resulted in reduced SSE decomposition and an improved first cycle Coulombic efficiency of 94%, from 84% when sulfide-based Li_3PS_4 was used[36].

Although studies using conventional cyclic voltammetry (CV) measurements have claimed SSE electrochemical stabilities up to 5 V or higher, recent reports using both modified CV measurements and first principles calculations have shown a narrower electrochemical voltage window. For example, LGPS, previously claimed to be stable up to 5 V with lithium metal[37], was found to decompose at 2.2 V versus Li/Li^+ (ref. [38,39]). These inconsistencies in stability were also found in oxide-based SSEs such as $Li_7La_3Zr_2O_{12}$ (LLZO) and $Li_{1+x}Al_xTi_{2-x}(PO_4)_3$ (LATP), where oxidative decomposition was reported to be higher (>5 V) than their predicted values (<3.7 V)[40,41]. These contradictory reports can be explained by the fact that experimental methods are sometimes unable to account for the sluggish redox kinetics of SSEs. In one example, instead of the common CV with metal current collectors, a modified process where SSE was mixed with carbon and applied on the cathode was consistent with the electrochemical stability windows derived from first principles calculations[39]. The use of carbon provides electronic pathways that facilitate redox of the SSE, allowing oxidation to be detected at its intrinsic thermodynamic potentials.

However, poor redox kinetics can in turn be applied to tune SSE oxidation. As decomposition products tend to deposit around the carbon additives or the surface of cathode particles, an ideal approach would involve minimizing SSE exposure to conductive surfaces, while providing long range electronic pathways between electrode materials and the current collector. As seen in Fig. 2c, the kinetics of SSE decomposition can be reduced by selecting a specific surface area of the carbon additives[42]. Carbon materials with low surface area (<100 $m^2\ g^{-1}$) and long range conductive capability, such as carbon nanotubes or vapour grown carbon fibre are ideal additives for ASSBs, because they reduce SSE decomposition and maintain high capacity utilization .

Characterization challenges

Challenges to characterize ASSBs often relate to the difficulty of probing buried and/or beam sensitive interfaces. Even though a wide spectrum of available tools exists, they are limited in characterizing specific chemistries within solid–solid interfaces. These include metallic lithium dendrites formation and growth of amorphous interfacial products within SSEs at both bulk and localized sites. Only in a few cases is it possible to characterize the true dynamic states within ASSBs with in situ and operando techniques. As such, recent reviews covering broad characterization topics have called for novel techniques to address this gap in knowledge[43–45]. In this section, we cover the state-of-the-art developments in experimental design for the characterization of ASSBs and offer possible solutions to address some of the most urgent problems.

Characterizing bulk ASSBs. To date, electrochemical methods such as galvanostatic cycling or impedance spectroscopy remain the primary characterization methods of buried interfaces within ASSBs[46]. However, such techniques are limited, because they cannot provide elemental or morphological information that are vital to properly evaluate cell failure mechanisms. Recently, X-ray computed tomography (CT) has been used to provide non-destructive three-dimensional (3D) in situ spatial visualization of dynamic morphological changes at solid–solid anodic interfaces[47]. Latest advancements in nano-CT capabilities (Fig. 3a) can achieve spatial resolutions below 50 nm over large sample volumes, potentially allowing the analysis of the entire cell packs. Unfortunately, poor X-ray absorption of lithium still makes it difficult to differentiate metallic lithium from sub-micron sized voids within the SSE. Thus, CT methods can be more effective when applied to cathodic interfaces where there is a larger X-ray contrast between cathode particles and SSEs. Several studies have quantified voids or cracks within the cathode composite using CT[48,49].

To probe buried interfaces, neutron-based techniques are especially useful. Neutron depth profiling (NDP) is effective to study lithium dendritic growth, as it is non-destructive and lithium-sensitive. In one example, cell shorting was diagnosed using NDP, where time-resolved lithium concentrations at the SSE–lithium interface were obtained as lithium was plated and stripped. It was found that increased accumulation of metallic lithium within the buried SSEs under high current densities was the likely cause for poor stripping reversibility and eventual cell shorting[50]. Another study used NDP to compare the dynamic evolution of lithium concentration in lithium–SSEs interfaces of LiPON, LLZO and Li_3PS_4 during Li plating. It was observed that lithium plating in LiPON remained uniform and unchanged throughout the process, in agreement with previous literature on lithium–LiPON interfaces. Microstructural lithium dendrite formation within buried SSEs can also be characterized using ^7Li nuclear magnetic resonance (NMR). Making use of non-destructive probes along with its high sensitivity toward Li^+ in bulk SSEs,^7Li NMR chemical shift imaging was used to track lithium growth in $Li_{6.5}La_3Zr_{1.5}Ta_{0.5}O_{12}$ (Fig. 3b). The increase in microstructural growths were subsequently correlated with symmetric cell plating and stripping voltage profiles, and it was found that voltage spikes often seen in ASSBs before cell failure can be attributed to dendrites that fuse (break) due to lithium melting during localized cell shorting[51]. However, the limited spatial resolution in such imaging techniques restricts detection to the micron-range (~100 μm). More sensitive techniques are needed to observe the initial onset of lithium nucleation, as these formations are likely to be nanometre-sized deposits within the SSEs.

Characterizing meso to nanoscale interfaces. To explore ASSB mesoscale properties, we need to revert to cryogenic focused ion beam (FIB) techniques (Fig. 3c). These methods can help quantify porosity and volume changes within the ASSBs at spatial resolutions under 1 nm without damaging the SSE or SEI. By keeping the sample temperatures low enough, local heating during exposure to Ga^+ ion beams can be prevented, allowing imaging of lithium metal at 100 K[52]. Considering the heterogeneous nature of the SEI layers, especially for thick electrodes, Xe^+ plasma FIB can be applied for large volume serial section tomography as the ion milling rates are at least 60 times greater than conventional Ga^+ FIB. Large volume tomography combined with windowless energy dispersive spectroscopy (EDS) can be used to monitor the SEI formation or cracking, electrode porosity and tortuosity evolution, and SEI layer elemental distribution changes in the 3D meso-structure. An example is illustrated in Fig. 3c where 3D reconstruction was used to quantify porosity as well as pores interconnectivity within an ASSB[53]. However, any reconstruction method using the FIB would be limited by the spatial resolutions of its detector—a scanning electron microscope (SEM) in this case. Additionally, the secondary electron signal intensities at cryogenic temperatures are low and charges from the probe beam can accumulate on electronically insulating SSEs, limiting the effectiveness of the method.

One strategy to overcome these challenges is the use of a solid-state nanobattery configuration for interface characterization (Fig. 3d). To do so, FIB is first used to slice a cross-sectional lamella from a thin-film ASSB. This lamella preserves the full function of the ASSB and is thin enough (~100 nm) to be used in a TEM. This approach was used to show electrochemical cyclability

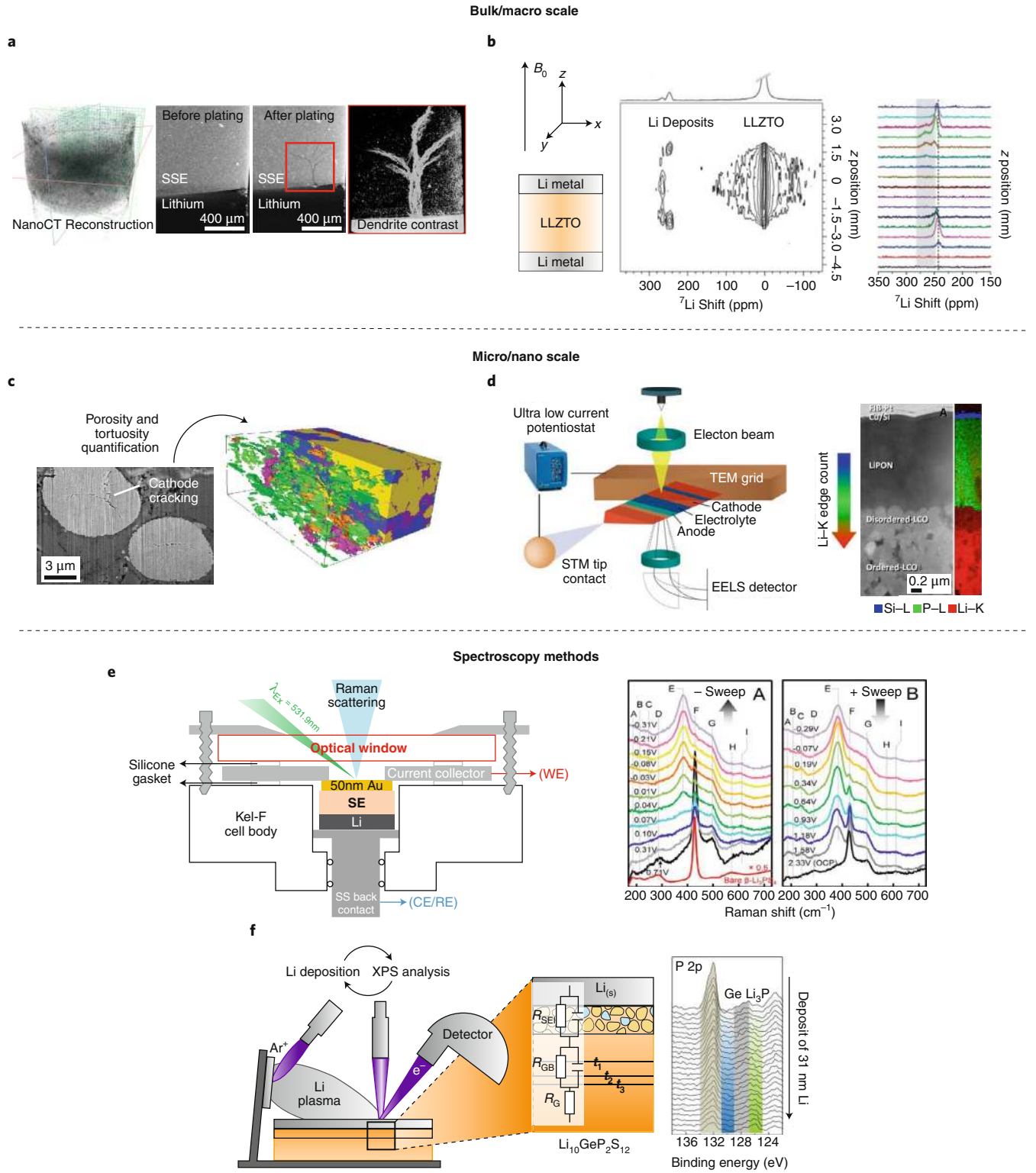

Fig. 3 | Summary of current effective methods to characterize all-solid-state batteries. a, Nano-computed tomography gives elemental contrast within buried solid electrolytes. **b**, ^{7}Li nuclear magnetic resonance chemical shift imaging observed lithium deposits within SSEs. LLZTO, tantalum doped lithium lanthanum zirconate garnet. **c**, Cryogenic focused ion/plasma beam reconstruction methods to quantify volume and porosity changes. **d**, Scanning transmission electron microscopy (STEM)/electron energy-loss spectroscopy (EELS) of nanobattery probing structural and chemical mapping of interfaces. **e**, In situ Raman spectroscopy tracks exchange of lithium thiophosphate units during plating and stripping. Kel-F, polychlorotrifluoroethylene; SS, stainless steel; WE, working electrode; CE, counter electrode; RE, reference electrode. **f**, In situ deposition of lithium on SSE coupled with X-ray photoelectron spectroscopy (XPS) showing decomposition progress. Panels **b**–**f** adapted with permission from refs. [19,51,53,86,87], American Chemical Society, in that order.

of a cross section LCO/LiPON/amorphous-Si thin film battery[54]. A wedge-shaped nano ASSB prepared by FIB was then placed onto a potentiostat coupled platform, allowing in situ cycling of the nano ASSB within the TEM. Using scanning TEM electron energy-loss spectroscopy (EELS), the decomposition products consisting of lithium oxides and peroxides and oxidized cobalt species could be observed at the cathode–SSE interface (Fig. 3d). Although such in situ TEM characterization has been demonstrated for thin-film LiPON based batteries, its principles can be applied for sulfide and oxide based ASSBs too, where sputtering or other vapour deposition methods can be used to fabricate nanobattery interfaces for the analysis.

Spectroscopy techniques. Various spectroscopy-based in situ methods have been adopted to probe electron beam sensitive and amorphous interfacial products. Of these, in situ Raman spectroscopy is a simple and robust method to provide good contrast in SSEs due to the strong scattering signals of covalently bonded interfacial products. With this technique, formation of various lithium thiophosphates, such as $P_2S_6^{4-}$ or PS_4^{3-}, can be easily distinguished during lithium plating at a gold–LGPS interface (Fig. 3e). Thiophosphate signals would otherwise be very difficult to distinguish with EELS, because this technique is sensitive to the P–S bond, which is present in both species. Limitations of in situ Raman include the inability to detect certain Raman inactive materials, especially ionic species such as lithium salts. Raman techniques also tend to be noisy especially from heterogeneous SSE interfaces, owing to the presence of absorbing or blocking materials such as carbon. One approach to overcome this issue is combining higher energy surface sensitive XPS with in situ deposition of lithium metal onto sulfide based LGPS (Fig. 3f). This allows detecting both chemical bonds and intrinsic band-structure, as well as observing the chemical decomposition products such as Li_3P, Li_2S, and Li—Ge alloy at the lithium –SSE interface[19]. However, its capability to capture subsurface (>10 nm) interfaces formation is limited by the escape depth of ejected photoelectrons. To address this issue, X-ray absorption spectroscopy (XAS) has been used in fluorescence mode to study oxidative decomposition of Li_3PS_4[54], where oxidized products of S and P_2S_5 were found in buried interface, in agreement with previous computational work[55].

Spectroscopy methods can also be utilized to qualitatively deconvolute chemical reactions from electrochemical reactions. This can be done through careful selection of their respective states of charge. For example, to probe chemical reactions between charged cathodes and SSEs without contributions from electrochemical decomposition, characterization can be conducted for mixtures of pristine SSEs and charged cathodes harvested from liquid electrolyte cells. Likewise, purely electrochemical reactions can be analyzed by characterizing SSE–carbon composites in the absence of transition metal oxide cathodes[55].

Scalable design—organic/inorganic composites

To achieve practical energy densities, SSE layers need to be thinner than 50 µm. However, the poor mechanical properties of inorganic SSEs makes them brittle, posing challenges for processing ASSBs in large formats. Polymer composites can improve mechanical flexibilities of SSE composites, allowing roll-to-roll manufacturing, with good elasticity and adhesion to current collectors.

Role of polymers in scalable fabrication. Figure 4a illustrates a typical manufacturing process of ASSBs using wet slurry processing methods similar to those in conventional LIBs[56]. However, unlike conventional LIBs manufacturing where common solvents such as water or N-methyl-2-pyrrolidone (NMP) and binders such as carboxymethyl cellulose (CMC) or polyvinylidene fluoride (PVDF) are used, careful consideration must be taken to ensure these solvents are chemically compatible with SSEs. While polyethylene oxide (PEO), polyvinylpyrrolidone (PVP), CMC and PVDF have been adopted in oxide-based ASSBs,[57,58] they cannot be used with sulfide-based SSEs. Electron-rich atoms within the polymer backbone, namely O, N and F, tend to form electrostatic interactions with the strong nucleophilic cations containing aliovalent atoms such as P or transition metals. This can result in localized SSE–binder agglomerations that impede both ionic conductivity and adhesive properties of the polymer. As such, favourable ASSB binders involve polymers with low or no electronegative functional groups, such as poly(acrylonitrile-co-butadiene) (NBR), polystyrene-block-polybutadiene (SBS) or styrene–ethylene–butylene–styrene (SEBS) reported in several cases; usually only 2 wt% of binder is needed to achieve sufficient adhesion[59–61]. While using non-polar binders may lead to poor adhesion between electrodes and current collectors, stack pressures typically applied in ASSBs can circumvent these concerns. Homogeneous electrode distribution is also a crucial factor for ASSBs, because poor particles wettability impedes capacity utilization. As such, binders that can be processed dry are promising candidates for ASSBs because they enable uniform distribution of the SSEs and active particles within the cathode composites[62].

Whenever solution processing is used, considerations for solvent and binders compatibility with sulfide-based SSEs must be made[63] (Fig. 4b). Only solvents with polarity index below 3.1 are fully compatible with sulfide-based SSEs[64]. In addition, the stability of the SSEs in ambient conditions needs to be considered. Sulfides spontaneously undergo hydrolysis when exposed to moisture, producing H_2S gas, a safety hazard when not properly vented. ASSB manufacturing should be done under dry-room conditions, similar to that of conventional LIBs. Trace amounts of moisture even in ppm levels can already be detrimental for the extremely hygroscopic sulfide SSEs. Studies have demonstrated improved moisture stability of sulfide SSEs using partial substitution of stable oxides into the bulk SSE[65]. Alternatively, to avoid modifying the intrinsic electrochemical properties of the SSE itself, hydrophobic binders can be adopted during processing[60].

Resistive effects of polymers. In general, it is expected that mixing a SSE with a binder decreases its conductivity by about an order of magnitude. This is due to the impedance contribution across the polymer–SSE interface as a result of the presence of insulating binder along the grain boundaries[61]. However, solvated ionic liquids (SILs) can reduce binder-induced impedance as well as fill any pore generated in the polymer composite. This strategy has been utilized to increase ionic conductivities by one to two orders of magnitude of oxide-based polymer–SSE composites[41,66]. However, this can be difficult to achieve in sulfide-based SSEs, as polar solvents that solvate lithium salts will chemically degrade the sulfides. This contradiction can be resolved by controlling the ratio between the salt and solvent. As the proportion of salt to solvent increases until saturation, a critical salt–solvent complex point is reached, forming a SIL with no available free solvent left to react with or dissolve sulfide SSEs. In an example, when four moles of triglyme G3 ethers were added to one mole of LiTFSI, a saturated solvent–salt complex, $Li(G3)_4$ was formed. This complex was found to not affect the sulfide SSE[67]. However, incorporation of any solvated ionic liquids in ASSBs such as LiG3 would also inevitably lower the thermal stability of the entire system. Thus, an alternative is the use of ionically conductive binders by solvating the insulating binders with lithium salts (Fig. 4c)[68]. In one case, a composite of Li_6PS_5Cl and NBR-Li(G3)TFSI solvated binder was applied[69], improving the cell rate capability and capacity utilization while maintaining good thermal stability. To eliminate the binder impedance contribution, binder-free ASSB cell fabrication has also been proposed. While binders play an important role during the manufacturing process, it is no longer needed once the cell is assembled. As a binder only acts as

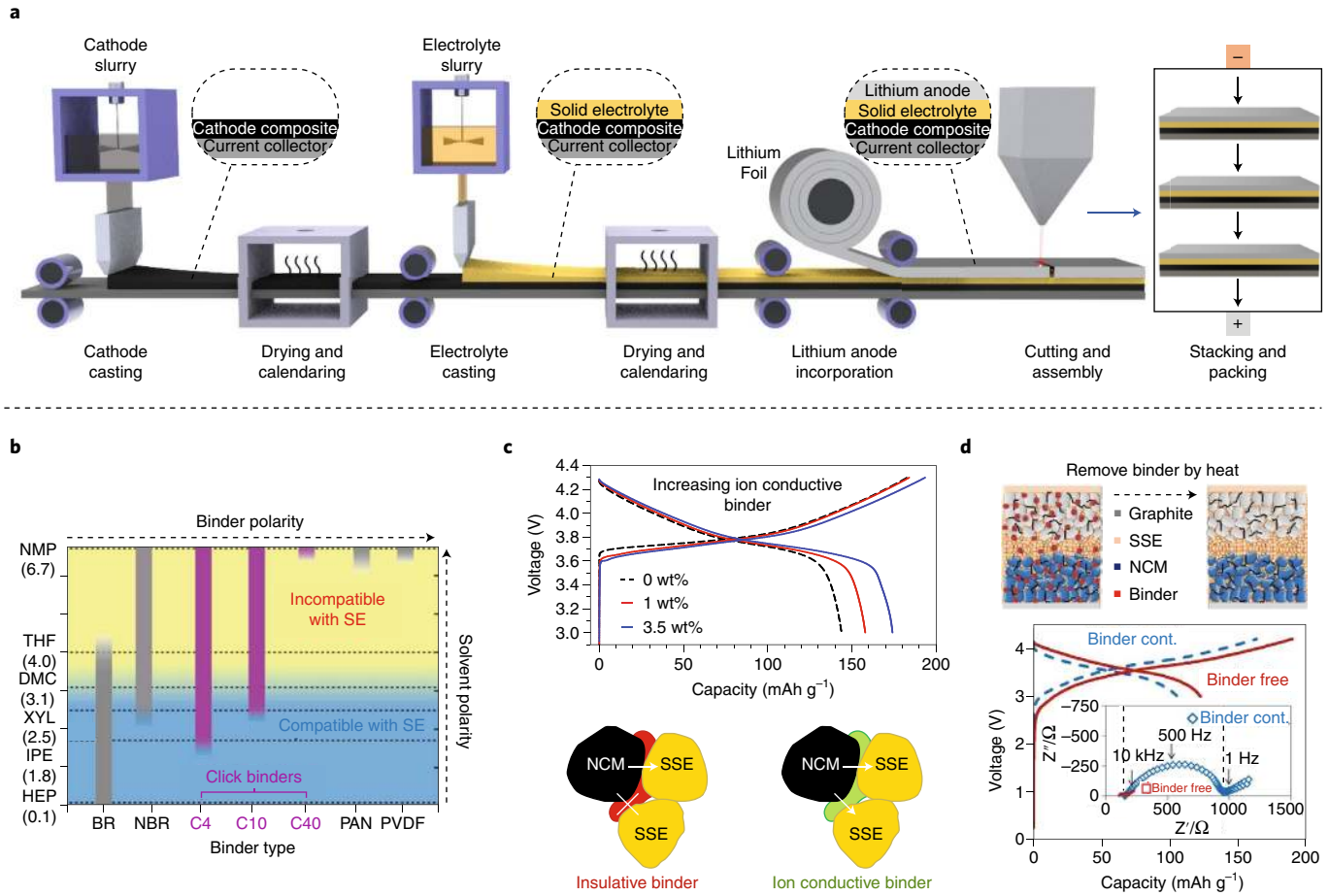

Fig. 4 | Manufacturing considerations for ASSBs and the role of polymeric binders. a, Schematic of large-scale manufacturing of ASSBs. Polymer and solid electrolyte composites allow for good mechanical processability as well as decreased separator thickness layers to increase cell-level energy density. **b**, Binder and solvent selection compatibility, showing the polarity window in which binders and solid electrolytes are compatible. BR, butadiene rubber; PAN, polyacrylonitrile; NMP, N-methyl-2-pyrrolidone; THF, tetrahydrofuran; DMC, dimethyl carbonate; XYL, xylene; IPE, isopropyl ether; HEP, heptane. C4, C10 and C40 refer to click binders with different degrees of grafting. **c**, Role of ionically conductive binder to improve conductive pathway and inter-particle contact. **d**, Binder-free cell fabrication reduces cell impedance and improves performance. Adapted with permission from ref. [64], American Chemical Society (**b**); ref. [69], Wiley (**c**); and ref. [70], CC BY 4.0 http://creativecommons.org/licenses/by/4.0/ (**d**).

inactive material, it would be ideal for it to be removed after assembly. Figure 4d depicts a heat treatment process that allows for the removal of volatile poly (propylene carbonate)-based binder within the cell after fabrication[70]. However, as the volume occupied by the binder is not filled by SSEs after removal, increased porosity within the ASSBs could potentially occur. As such, this temperature treatment technique can be done under stack pressure, allowing the thermally softened SSEs to deform and fill any pores generated within the solid electrolyte bulk.

Battery recycling and sustainability

With rapidly increased LIBs adoption, the need for sustainable battery recycling is a matter of utmost importance. Spent LIBs contain lithium, cobalt, nickel and other transition metals that are not only economically valuable but are also limited in terms of their natural availabilities. Unfortunately, today's LIBs are not designed to be recycled easily[71]. To re-design batteries for recycling instead of disposal, battery manufacturers will need to modify their established production protocols, with evident economic backslash. While this might be too late for conventional LIBs, it is prudent to design potential recycling strategies such that future ASSB manufacturers can consider it as part of a sustainable production-to-recycling manufacturing process.

Battery recycling challenges. Figure 5a depicts the battery manufacturing chain from materials mining to disposal. While recycling efficiencies for lead acid batteries exceed 99% in major parts of the world[72], such as in Europe and the USA where recycling is led by strong government mandates, much more can be done to improve recycling rates for end-of-life LIBs and future ASSBs. Moreover, commercial LIBs should be regulated to include labelling of their chemical classifications, to allow ease of recycling and sorting based on their core materials. This would require the co-operation of battery manufacturers and policy makers, in efforts to streamline recycling of respective LIB chemistries. The responsibility can be further extended to original equipment manufacturers as well as EV manufacturers to incentivize battery buy-back programmes as part of their in-house recycling or repackaging for secondary use.

The most common recycling technologies adopted today to break down recovered cathode materials and regenerate them for reuse are pyrometallurgical and hydrometallurgical methods. Recent studies on such methods have reported valuable metal recovery rates exceeding 95% using acid leaching followed by chemical precipitation methods[73–75]. The recovered metals in their precursor forms are subsequently used in cathode re-synthesis with co-precipitation, sol-gel or solid-state heat treatment steps to reform the active materials.

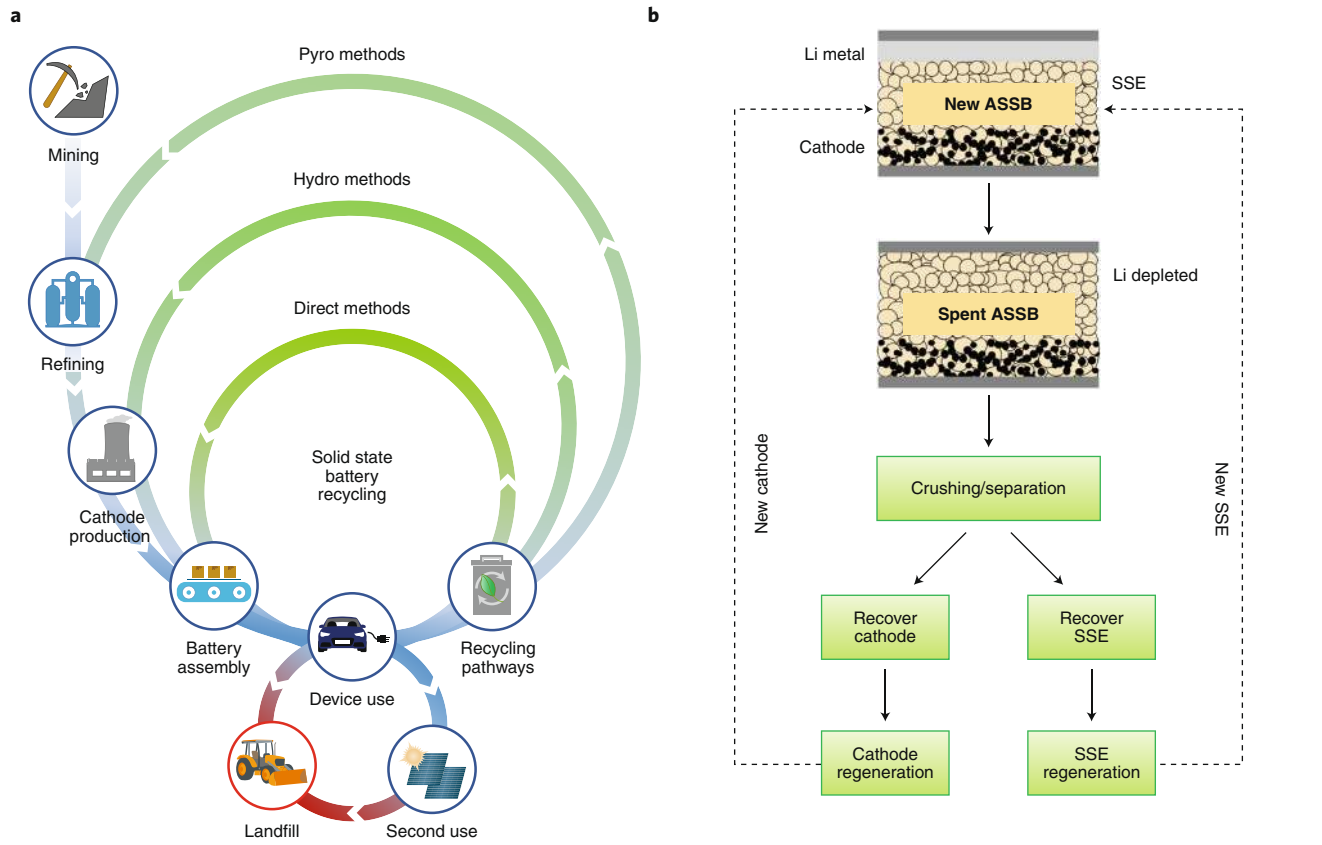

Fig. 5 | Strategies toward sustainable battery recycling. a, Illustration of various recycling methods with reference to direct battery recycling method proposed in solid state batteries. **b**, Schematic of potential closed loop all-solid-state battery direct recycling process. Panel **a** adapted with permission from https://recellcenter.org/research, Argonne National Laboratory (managed and operated by UChicago Argonne, LLC, for the US Department of Energy under contract no. DEAC02- 06CH11357).

However, these methods tend to be energy intensive, costly and use toxic chemicals processing, which can be difficult to handle[76]. Additionally, materials recovery efficiency as a fraction of the entire cell still remains low, due to low recycling rates of other components in the cell such as the liquid electrolytes, lithium salts, separator and additives. To address these shortcomings, the US Department of Energy's ReCell Center has set out core principles of battery recycling that involves design for recyclability, direct regeneration and recovery of other components (https://recellcenter.org/research). Achieving these goals requires a paradigm shift in the way researchers think about battery recycling, to go beyond metals recovery or materials processability, and to consider LIBs and ASSBs recycling from a wider perspective[75]. Given the lack of reports on ASSBs recycling in the literature, this framework presents an opportunity to explore possible pathways for recycling ASSBs using the goals of ReCell as a starting reference point.

Fully recyclable ASSB model. For any ASSB recycling model to be sustainable and practical, several technical challenges need to be addressed: (1) designing ASSB cell chemistries that allow for efficient materials disassembly with reduced processing steps; (2) avoid using toxic, expensive and difficult-to-process organic solvents; (3) recovering all components in a battery, rather than just the cathode, in a cost-effective manner; and (4) designing a scalable, closed loop ASSB recycling model applicable to a variety of ASSB formats (Fig. 5b).

Fortunately, compared to conventional liquid-electrolyte-based LIBs, recycling of ASSBs has several advantages. Due to its large stackable formats, ASSBs can be discharged at the pack level before disassembly; and its intrinsic non-flammability also mitigates safety hazards during packaging breakdown. Conversely, fire and gas evolution hazards in LIBs require individual cells to be submerged typically in salt solution to achieve zero state of charge. However, the major challenge for a recyclable ASSB model is separation of SSEs from electrodes and its subsequent recovery. Unlike liquid electrolytes that can be removed with organic solvents or supercritical drying during dismantling[74,77], SSEs contains a host of various metallic and non-metallic elements (oxides, sulfides). Elemental separation and purification of these SSEs can be difficult with conventional recycling approaches. While solution type dissolution and precipitation methods of SSEs might be effective, the fact that transition-metal oxide chemistries are similar in both oxide-based SSEs and cathode materials make it challenging to selectively separate each component via dissolution. Fortunately, this should not be the case in sulfide-based ASSBs, where sulfide dissolution can be done using cheap and safe solvents such as ethanol or acetonitrile to recover sulfide-based SSEs from spent ASSBs[78]. Unlike previous studies that reported chemical incompatibilities between polar solvents and sulfides[64], it has been found that such polar solvents will only cause dissolution and not chemical degradation of certain SSEs, allowing them to be precipitated in its original chemical formula. Solution-based processing of sulfide-based SSEs using such solvents has been already demonstrated in previous solution synthesis work[79–81]. This is often seen in sulfide-based SSEs comprising of PS_4^{3-} conductive thiophosphate units that can be easily solvated with polar solvents and precipitated as either Li_3PS_4 or Li_6PS_5X (X = Cl, Br or I) forms. By contrast, conventional LIB cells need to be separated into their subcomponents before washing away the electrolyte solvents and

salts. Moreover, ASSBs contain no ethers, salts or separators and its SSEs can potentially be fully recovered without energy intensive organics processing. This provides a promising opportunity for simple recovery and recycling of SSEs from spent ASSBs.

Direct regeneration of SSEs and cathodes. A crucial requirement for any robust recycling model is the need to avoid the breakdown of spent electrodes and SSEs to their precursor forms. As such, direct regeneration methods would be superior to existing energy intensive pyrometallurgical or hydrometallurgical methods, as they substantially reduce the energy and processing costs of recycling. Conceptually, spent bulk SSEs do not undergo any structural change aside from fractional decomposition in the SEI. Thus, the majority of the SSE can be recovered and directly regenerated without sophisticated re-synthesis processes using dissolution–precipitation methods combined with mild post processing. Although sulfide SSE dissolution processes can result in conductivity losses of 1 to 2 orders of magnitude[79,80], this is mainly due to the small grain sizes and poor crystallinity of recovered SSEs, not to chemical degradation of the SSE itself. It has been shown that mild annealing can be carried out for precipitated SSEs to regain its pure phase and ionic conductivities greater than 1 mS cm^{-1} (refs. [79,80]). Such techniques can allow simple and low-cost recovery of lithium in its reusable SSE form.

Aside from the SSE, direct regeneration of spent electrodes is also possible. Previous nanoscale characterization work done on aged LIBs has shown that the degradation of transition metal oxides occurs mainly on the surface or subsurface, forming localized spinel or rock salt phases[82]. Therefore, total destruction and recovery of the bulk cathode are not necessary. Recent reports on direct re-lithiation of spent layered oxides (LCO, NMC) via solution, solid state and molten salt infusion methods provide promising approaches for cathode direct regeneration[83,84]. As an end-of-life lithium metal ASSB would be fully depleted of lithium, or contain only traces of unconsumed lithium (Fig. 5b), recycling strategies can be centred around processing the SSE and surface degraded cathodes. Although cathode coating materials used in ASSBs such as $LiNbO_3$ would remain on the surface of cathodes, direct regeneration using re-lithiation methods can be done together with these ionically conductive coating layers that facilitate Li^+ diffusion. This eliminates the need to break down either the protective coating layers or bulk cathode into precursors forms. Once the correct stoichiometric ratio of lithium and transition metals are achieved, annealing can be done to reach the target crystal structure and removal of any remaining impurities. While existing studies on SSE solution processing and cathode direct regeneration have demonstrated the technical feasibility of recycling an end-of-life ASSB, this has yet to be tested in a full-cell pack. However, the proposed recycling model here may provide potential ASSB manufacturers new strategies for future sustainable battery designs, lowering financial burdens of manufacturing environmentally friendly commercialized ASSBs without compromising energy density and overall cell performance.

Conclusions

The continued pursuit of sustainable energy storage technologies with increasing energy density and safety demands will compel an inevitable shift from conventional LIBs to ASSBs. Developing a single type of SSE capable of meeting all required properties remains challenging, but the combination of materials and nano-engineering shows great promise toward overcoming obstacles such as interfacial stability by controlling the thermodynamics and kinetics of SSE decomposition. We have highlighted the state-of-the-art characterization techniques to shed light onto the nano-scale phenomena within buried SSE interfaces and have proposed methods for in situ observation of unstable solid–solid interfaces. We have also discussed polymer–SSE composites, solvent–polymer combination selection criteria, and methods to reduce resistive effects of binders. The aim is to accelerate commercialization of ASSBs using scalable solution-based processes. Finally, we have introduced strategies for sustainable ASSBs recycling, and proposed a fully recyclable ASSB model that can potentially lower costs of battery recycling with safer and simpler methods compared to current technologies. Nanotechnology itself may not be an all-encompassing silver bullet for every challenge faced by ASSBs, however it is certainly becoming an enabler for deeper understanding of nanoscale phenomena, helping better design strategies that can translate into improvements in materials and cell level performance.

Received: 11 June 2019; Accepted: 11 February 2020;
Published online: 10 March 2020

References

1. Yu, C. et al. Facile synthesis toward the optimal structure-conductivity characteristics of the argyrodite Li_6PS_5Cl solid-state electrolyte. *ACS Appl. Mater. Interfaces* **10**, 33296–33306 (2018).
2. Nguyen, H. et al. Single-step synthesis of highly conductive Na_3PS_4 solid electrolyte for sodium all solid-state batteries. *J. Power Sources* **435**, 126623 (2019).
3. Kato, Y. et al. High-power all-solid-state batteries using sulfide superionic conductors. *Nat. Energy* **1**, 16030 (2016).
4. Zhu, Y., He, X. & Mo, Y. Origin of outstanding stability in the lithium solid electrolyte materials: insights from thermodynamic analyses based on first-principles calculations. *ACS Appl. Mater. Interfaces* **7**, 23685–23693 (2015).
5. Zhang, H. et al. Single lithium-ion conducting solid polymer electrolytes: advances and perspectives. *Chem Soc Rev* **46**, 797–815 (2017).
6. Mindemark, J., Lacey, M. J., Bowden, T. & Brandell, D. Beyond PEO—alternative host materials for Li^+ conducting solid polymer electrolytes. *Prog. Polym. Sci.* **81**, 114–143 (2018).
7. Yao, P. et al. Review on polymer-based composite electrolytes for lithium batteries. *Front. Chem.* **7**, 522 (2019).
8. Auvergniot, J. et al. Interface stability of argyrodite Li_6PS_5Cl toward $LiCoO_2$, $LiNi_{1/3}Co_{1/3}Mn_{1/3}O_2$, and $LiMn_2O_4$ in bulk all-solid-state batteries. *Chem. Mater.* **29**, 3883–3890 (2017).
9. Auvergniot, J. et al. Redox activity of argyrodite Li_6PS_5Cl electrolyte in all-solid-state Li-ion battery: an XPS study. *Solid State Ionics* **300**, 78–85 (2017).
10. Haruyama, J., Sodeyama, K., Han, L., Takada, K. & Tateyama, Y. Space–charge layer effect at interface between oxide cathode and sulfide electrolyte in all-solid-state lithium-ion battery. *Chem. Mater.* **26**, 4248–4255 (2014).
11. Ohta, N. et al. Enhancement of the high-rate capability of solid-state lithium batteries by nanoscale interfacial modification. *Adv. Mater.* **18**, 2226–2229 (2006).
12. Li, X. et al. $LiNbO_3$-coated $LiNi_{0.8}Co_{0.1}Mn_{0.1}O_2$ cathode with high discharge capacity and rate performance for all-solid-state lithium battery. *J. Energy Chem.* **40**, 39–45 (2019).
13. Haruyama, J., Sodeyama, K. & Tateyama, Y. Cation mixing properties toward Co diffusion at the $LiCoO_2$ cathode/sulfide electrolyte interface in a solid-state battery. *ACS Appl. Mater. Interfaces* **9**, 286–292 (2017).
14. Sakuda, A., Hayashi, A. & Tatsumisago, M. Interfacial observation between $LiCoO_2$ electrode and $li_2s–p_2s_5$ solid electrolytes of all-solid-state lithium secondary batteries using transmission electron microscopy. *Chem. Mater.* **22**, 949–956 (2010).
15. Woo, J. H. et al. Nanoscale interface modification of $LiCoO_2$ by Al_2O_3 atomic layer deposition for solid-state li batteries. *J. Electrochem. Soc.* **159**, A1120–A1124 (2012).
16. Okada, K. et al. Preparation and electrochemical properties of $LiAlO_2$ coated $Li(Ni_{1/3}Mn_{1/3}Co_{1/3})O_2$ for all-solid-state batteries. *Solid State Ionics* **255**, 120–127 (2014).
17. Xiao, Y., Miara, L. J., Wang, Y. & Ceder, G. Computational Screening of Cathode Coatings for Solid-State. *Batteries. Joule* **3**, 1252–1275 (2019).
18. Koerver, R. et al. Capacity fade in solid-state batteries: interphase formation and chemomechanical processes in nickel-rich layered oxide cathodes and lithium thiophosphate solid electrolytes. *Chem. Mater.* **29**, 5574–5582 (2017).
19. Wenzel, S. et al. Direct observation of the interfacial instability of the fast ionic conductor $Li_{10}GeP_2S_{12}$ at the lithium metal anode. *Chem. Mater.* **28**, 2400–2407 (2016).
20. Han, X. et al. Negating interfacial impedance in garnet-based solid-state Li metal batteries. *Nat. Mater.* **16**, 572–579 (2017).
21. Yersak, T., Salvador, J. R., Schmidt, R. D. & Cai, M. Hot pressed, fiber-reinforced $(Li_2S)70(P_2S_5)30$ solid-state electrolyte separators for Li metal batteries. *ACS Appl. Energy Mater.* **2**, 3523–3531 (2019).

22. Kim, S. H. et al. In situ observation of lithium metal plating in a sulfur-based solid electrolyte for all-solid-state batteries. *J. Mater. Chem. A* **7**, 13650–13657 (2019).
23. Tao, X. et al. Solid-state lithium-sulfur batteries operated at 37 °C with composites of nanostructured $Li_7La_3Zr_2O_{12}$/carbon foam and polymer. *Nano Lett.* **17**, 2967–2972 (2017).
24. Ates, T., Keller, M., Kulisch, J., Adermann, T. & Passerini, S. Development of an all-solid-state lithium battery by slurry-coating procedures using a sulfidic electrolyte. *Energy Storage Mater.* **17**, 204–210 (2019).
25. Han, F., Yue, J., Zhu, X. & Wang, C. Suppressing Li dendrite formation in Li_2S-P_2S_5 solid electrolyte by LiI incorporation. *Adv. Energy Mater.* **8**, 1703644 (2018).
26. Li, Y. et al. Mastering the interface for advanced all-solid-state lithium rechargeable batteries. *Proc. Natl Acad. Sci. USA* **113**, 13313–13317 (2016).
27. Kerman, K., Luntz, A., Viswanathan, V., Chiang, Y.-M. & Chen, Z. Review—practical challenges hindering the development of solid state Li ion batteries. *J. Electrochem. Soc.* **164**, A1731–A1744 (2017).
28. Aguesse, F. et al. Investigating the dendritic growth during full cell cycling of garnet electrolyte in direct contact with Li metal. *ACS Appl. Mater. Interfaces* **9**, 3808–3816 (2017).
29. Swamy, T. et al. Lithium metal penetration induced by electrodeposition through solid electrolytes: example in single-crystal $Li_6La_3ZrTaO_{12}$ garnet. *J. Electrochem. Soc.* **165**, A3648–A3655 (2018).
30. Neudecker, B. J., Dudney, N. J. & Bates, J. B. "Lithium-free" thin-film battery with in situ plated Li snode. *J. Electrochem. Soc.* **147**, 517–523 (2000).
31. Li, J., Ma, C., Chi, M., Liang, C. & Dudney, N. J. Solid electrolyte: the key for high-voltage lithium batteries. *Adv. Energy Mater.* **5**, 1401408 (2015).
32. Fang, C. et al. Quantifying inactive lithium in lithium metal batteries. *Nature* **572**, 511–515 (2019).
33. Sharafi, A. et al. Surface chemistry mechanism of ultra-low interfacial resistance in the solid-state electrolyte $Li_7La_3Zr_2O_{12}$. *Chem. Mater.* **29**, 7961–7968 (2017).
34. Tao, Y. et al. Lithium superionic conducting oxysulfide solid electrolyte with excellent stability against lithium metal for all-solid-state cells. *J. Electrochem. Soc.* **163**, A96–A101 (2016).
35. Sun, Y. et al. Oxygen substitution effects in $Li_{10}GeP_2S_{12}$ solid electrolyte. *J. Power Sources* **324**, 798–803 (2016).
36. Asano, T. et al. Solid halide electrolytes with high lithium-ion conductivity for application in 4 V class bulk-type all-solid-state batteries. *Adv. Mater.* **30**, e1803075 (2018).
37. Kamaya, N. et al. A lithium superionic conductor. *Nat. Mater.* **10**, 682–686 (2011).
38. Han, F., Zhu, Y., He, X., Mo, Y. & Wang, C. Electrochemical stability of $Li_{10}GeP_2S_{12}$ and $Li_7La_3Zr_2O_{12}$ solid electrolytes. *Adv. Energy Mater.* **6**, 1501590 (2016).
39. Han, F., Gao, T., Zhu, Y., Gaskell, K. J. & Wang, C. A battery made from a single material. *Adv. Mater.* **27**, 3473–3483 (2015).
40. Yan, X., Li, Z., Wen, Z. & Han, W. Li/$Li_7La_3Zr_2O_{12}$/$LiFePO_4$ All-solid-state battery with ultrathin nanoscale solid electrolyte. *J. Phys. Chem. C* **121**, 1431–1435 (2017).
41. Shi, X. et al. Fabrication and electrochemical properties of LATP/PVDF composite electrolytes for rechargeable lithium-ion battery. *Solid State Ion.* **325**, 112–119 (2018).
42. Zhang, W. et al. The detrimental effects of carbon additives in $Li_{10}GeP_2S_{12}$ based solid-state batteries. *ACS Appl. Mater. Interfaces* **9**, 35888–35896 (2017).
43. Xu, L. et al. Interfaces in solid-state lithium batteries. *Joule* **2**, 1991–2015 (2018).
44. Lewis, J. A., Tippens, J., Cortes, F. J. Q. & McDowell, M. T. Chemo-mechanical challenges in solid-state batteries. *Trends Chem.* **1**, 845–857 (2019).
45. Manthiram, A., Yu, X. & Wang, S. Lithium battery chemistries enabled by solid-state electrolytes. *Nat. Rev. Mater.* **2**, 16103 (2017).
46. Ren, Y., Shen, Y., Lin, Y. & Nan, C.-W. Direct observation of lithium dendrites inside garnet-type lithium-ion solid electrolyte. *Electrochem. Commun.* **57**, 27–30 (2015).
47. Seitzman, N. et al. Toward all-solid-state lithium batteries: three-dimensional visualization of lithium migration in β-Li_3PS_4 ceramic electrolyte. *J. Electrochem. Soc.* **165**, A3732–A3737 (2018).
48. Li, T. et al. Three-dimensional reconstruction and analysis of all-solid Li-ion battery electrode using synchrotron transmission X-ray microscopy tomography. *ACS Appl. Mater. Interfaces* **10**, 16927–16931 (2018).
49. Chen-Wiegart, Y.-cK., Liu, Z., Faber, K. T., Barnett, S. A. & Wang, J. 3D analysis of a $LiCoO_2$–$Li(Ni_{1/3}Mn_{1/3}Co_{1/3})O_2$ Li-ion battery positive electrode using x-ray nano-tomography. *Electrochem. Commun.* **28**, 127–130 (2013).
50. Wang, C. et al. In situ neutron depth profiling of lithium metal-garnet interfaces for solid state batteries. *J. Am. Chem. Soc.* **139**, 14257–14264 (2017).
51. Marbella, L. E. et al. ^{7}Li NMR chemical shift imaging to detect microstructural growth of lithium in all-solid-state batteries. *Chem. Mater.* **31**, 2762–2769 (2019).
52. Lee, J. Z. et al. Cryogenic focused ion beam characterization of lithium metal anodes. *ACS Energy Lett.* **4**, 489–493 (2019).
53. Choi, S. et al. Quantitative analysis of microstructures and reaction interfaces on composite cathodes in all-solid-state batteries using a three-dimensional reconstruction technique. *ACS Appl. Mater. Interfaces* **10**, 23740–23747 (2018).
54. Santhanagopalan, D. et al. Interface limited lithium transport in solid-state batteries. *J. Phys. Chem. Lett.* **5**, 298–303 (2014).
55. Hakari, T. et al. Structural and electronic-state changes of a sulfide solid electrolyte during the Li deinsertion–insertion processes. *Chem. Mater.* **29**, 4768–4774 (2017).
56. Schnell, J. et al. All-solid-state lithium-ion and lithium metal batteries – paving the way to large-scale production. *J. Power Sources* **382**, 160–175 (2018).
57. Zhang, X. et al. Synergistic coupling between $Li_{6.75}La_3Zr_{1.75}Ta_{0.25}O_{12}$ and poly(vinylidene fluoride) induces high ionic conductivity, mechanical strength, and thermal stability of solid composite electrolytes. *J. Am. Chem. Soc.* **139**, 13779–13785 (2017).
58. Jung, Y.-C., Lee, S.-M., Choi, J.-H., Jang, S. S. & Kim, D.-W. All Solid-State Lithium Batteries Assembled with Hybrid Solid Electrolytes. *J. Electrochem. Soc.* **162**, A704–A710 (2015).
59. Nam, Y. J., Oh, D. Y., Jung, S. H. & Jung, Y. S. Toward practical all-solid-state lithium-ion batteries with high energy density and safety: comparative study for electrodes fabricated by dry- and slurry-mixing processes. *J. Power Sources* **375**, 93–101 (2018).
60. Tan, D. H. S. et al. Enabling thin and flexible solid-state composite electrolytes by the scalable solution process. *ACS Appl. Energy Mater.* **2**, 6542–6550 (2019).
61. Sakuda, A. et al. All-solid-state battery electrode sheets prepared by a slurry coating process. *J. Electrochem. Soc.* **164**, A2474–A2478 (2017).
62. Hippauf, F. et al. Overcoming binder limitations of sheet-type solid-state cathodes using a solvent-free dry-film approach. *Energy Storage Mater.* **21**, 390–398 (2019).
63. Lee, K. et al. Selection of binder and solvent for solution-processed all-solid-state battery. *J. Electrochem. Soc.* **164**, A2075–A2081 (2017).
64. Lee, K., Lee, J., Choi, S., Char, K. & Choi, J. W. Thiol–ene click reaction for fine polarity tuning of polymeric binders in solution-processed all-solid-state batteries. *ACS Energy Lett.* **4**, 94–101 (2018).
65. Hayashi, A., Muramatsu, H., Ohtomo, T., Hama, S. & Tatsumisago, M. Improvement of chemical stability of Li_3PS_4 glass electrolytes by adding MxOy (M = Fe, Zn, and Bi) nanoparticles. *J. Mater. Chem. A* **1**, 6320 (2013).
66. Liang, X., Han, D., Wang, Y., Lan, L. & Mao, J. Preparation and performance study of a PVDF–LATP ceramic composite polymer electrolyte membrane for solid-state batteries. *RSC Adv.* **8**, 40498–40504 (2018).
67. Oh, D. Y. et al. Excellent compatibility of solvate ionic liquids with sulfide solid electrolytes: toward favorable ionic contacts in bulk-type all-solid-state lithium-ion batteries. *Adv. Energy Mater.* **5**, 1500865 (2015).
68. Zeng, X., Li, J. & Ren, Y. Prediction of various discarded lithium batteries in china. In *Proc. IEEE International Symposium on Sustainable Systems and Technology (ISSST)* 1–4 (IEEE, 2012).
69. Oh, D. Y. et al. Slurry-fabricable Li^+ conductive polymeric binders for practical all-solid-state lithium-ion batteries enabled by solvate ionic liquids. *Adv. Energy Mater.* **9**, 1802927 (2019).
70. Yamamoto, M., Terauchi, Y., Sakuda, A. & Takahashi, M. Binder-free sheet-type all-solid-state batteries with enhanced rate capabilities and high energy densities. *Sci. Rep.* **8**, 1212 (2018).
71. Xu, J. et al. A review of processes and technologies for the recycling of lithium-ion secondary batteries. *J. Power Sources* **177**, 512–527 (2008).
72. May, G. J., Davidson, A. & Monahov, B. Lead batteries for utility energy storage: a review. *J. Energy Storage* **15**, 145–157 (2018).
73. Zhang, X. et al. Toward sustainable and systematic recycling of spent rechargeable batteries. *Chem. Soc. Rev.* **47**, 7239–7302 (2018).
74. Li, L. et al. The recycling of spent lithium-ion batteries: a review of current processes and technologies. *Electrochem. Energy Rev.* **1**, 461–482 (2018).
75. Liu, T. et al. Sustainability-inspired cell design for a fully recyclable sodium ion battery. *Nat. Commun.* **10**, 1965 (2019).
76. Zheng, X. et al. A mini-review on metal recycling from spent lithium ion batteries. *Engineering* **4**, 361–370 (2018).
77. Nowak, S. & Winter, M. The role of sub- and supercritical CO_2 as "Processing Solvent" for the recycling and sample preparation of lithium ion battery electrolytes. *Molecules* **22**, 403 (2017).
78. Miura, A. et al. Liquid-phase syntheses of sulfide electrolytes for all-solid-state lithium battery. *Nat. Rev. Chem.* **3**, 189–198 (2019).

79. Wang, Y. et al. Mechanism of formation of $Li_7P_3S_{11}$ solid electrolytes through liquid phase synthesis. *Chem. Mater.* **30**, 990–997 (2018).
80. Kim, D. H. et al. Infiltration of solution-processable solid electrolytes into conventional Li-Ion-battery electrodes for all-solid-state Li-Ion batteries. *Nano Lett* **17**, 3013–3020 (2017).
81. Calpa, M., Rosero-Navarro, N. C., Miura, A. & Tadanaga, K. Instantaneous preparation of high lithium-ion conducting sulfide solid electrolyte $Li_7P_3S_{11}$ by a liquid phase process. *RSC Adv.* **7**, 46499–46504 (2017).
82. Jung, S.-K. et al. Understanding the degradation mechanisms of $LiNi_{0.5}Co_{0.2}Mn_{0.3}O_2$ cathode material in lithium ion batteries. *Adv. Energy Mater.* **4**, 1300787 (2014).
83. Zhang, X. et al. sustainable recycling and regeneration of cathode scraps from industrial production of lithium-ion batteries. *ACS Sustainable Chem. Eng.* **4**, 7041–7049 (2016).
84. Shi, Y., Zhang, M., Meng, Y. S. & Chen, Z. Ambient-pressure relithiation of degraded $Li_xNi_{0.5}Co_{0.2}Mn_{0.3}O_2$ ($0 < x < 1$) via eutectic solutions for direct regeneration of lithium-ion battery cathodes. *Adv. Energy Mater.* **9**, 1900454 (2019).
85. Wang, S. et al. Lithium chlorides and bromides as promising solid-state chemistries for fast ion conductors with good electrochemical stability. *Angew. Chem. Int. Ed.* **58**, 8039–8043 (2019).
86. Wang, Z. et al. In situ STEM-EELS observation of nanoscale interfacial phenomena in all-solid-state batteries. *Nano Lett.* **16**, 3760–3767 (2016).
87. Sang, L., Haasch, R. T., Gewirth, A. A. & Nuzzo, R. G. Evolution at the solid electrolyte/gold electrode interface during lithium deposition and stripping. *Chem. Mater.* **29**, 3029–3037 (2017).

Acknowledgements

This work was financially supported by the LG Chem through the Battery Innovation Contest (BIC) program as well as the Energy & Biosciences Institute through the EBI-Shell program. Z.C. acknowledges funding from the US Department of Energy via ReCell Center and the start-up fund support from the Jacob School of Engineering at University of California San Diego. Y.S.M. acknowledges the funding support from Zable Endowed Chair Fund.

Competing interests

The authors declare no competing financial interests.

Additional information

Correspondence should be addressed to Z.C. or Y.S.M.

Reprints and permissions information is available at www.nature.com/reprints.

Publisher's note Springer Nature remains neutral with regard to jurisdictional claims in published maps and institutional affiliations.